43rd AIAA/ASME/SAE/ASEE Joint Propulsion Conference & Exhibit
8 - 11 July 2007, Cincinnati, OH

AIAA 2007-5208

Shear-Based Model for Electron Transport in 2D Hybrid Hall Thruster Simulations

Michelle K. Scharfe*, Cliff A. Thomas*, David B. Scharfe*, Nicolas Gascon†, and Mark A. Cappelli‡

Stanford University, Stanford, CA, 94305

Eduardo Fernandez§

Eckerd College, St. Petersburg, FL, 33711

An electron cross-field transport model based on instantaneous simulated plasma properties is incorporated into a radial-axial hybrid simulation of a Hall plasma accelerator. The model is used to capture the reduction of fluctuation-based anomalous transport in the region of high axial shear of the electron fluid. Similar transport barriers are observed in the fusion community due to shear suppression of plasma turbulence through an increase in the decorrelation rate of plasma eddies. A comparison is made between shear-based, experimental, and Bohm-type models for cross-field transport. The sensitivity of the shear-based transport model to fitting parameters and the transportability of these parameters to other operating conditions are examined.

Nomenclature

E Electric field
B Magnetic field
u Velocity
s Shear rate
$\omega\tau$ Hall parameter

Subscript
e Electron
eff Effective
$clas$ Classical
nw Near wall
$fluc$ Fluctuation
r Radial direction
z Axial direction
θ Azimuthal direction

I. Introduction

The future capability of space exploration is dependent on the development of electric propulsion devices. While the high thrust provided by chemical rockets is necessary for escape from the Earth's strong gravitational pull, operations such as satellite station keeping and orbit transfer can be more efficiently accomplished using plasma thrusters. Also, the continuous, low thrust, high specific impulse provided by

*Research Assistant, Mechanical Engineering Department, MC 3032, Member AIAA.
†Research Associate, Mechanical Engineering Department, MC 3032, Member AIAA.
‡Professor, Mechanical Engineering Department, MC 3032, Member AIAA.
§Associate Professor, Mathematics and Physics.

these devices is of immense value to missions of exploration and discovery. In addition to achieving higher maximum velocities than chemical propulsion for long duration missions, electric propulsion also provides greater trajectory control allowing for longer and more precise observation of desired targets.

The efficient operation of electric propulsion devices relies on their ability to ionize neutral gas and accelerate the ionized particles to high exhaust velocities using electric and magnetic fields. In a coaxial Hall effect thruster, ions are accelerated using an externally applied electric field, while electrons are trapped in a region of strong magnetic field by an azimuthal E×B Hall current. The mechanism by which electrons traverse magnetic field lines is an area of considerable research. Experimentally, the electron conductivity in these devices is observed to be higher than predicted based on electron collisions with heavy particles.[1] Possible explanations for the anomalous conductivity are near wall transport[2,3] and azimuthal fluctuations,[4] both of which increase the effective collision frequency of electrons.

An accurate model for electron transport is critical for the development of a Hall thruster simulation with predictive capabilities. One common method for describing anomalous cross field transport involves using a fluctuation based Bohm-type model that scales inversely with the magnetic field (unlike the $1/B^2$ dependence of the classical collision model). While this method is in reasonable agreement with experiment for most regions of the thruster channel, there exists a region near the peak in magnetic field where the electron mobility is experimentally observed to be nearly classical. This region of lower electron conductivity, which occurs in a region of strong gradients, is somewhat paradoxical in that instabilities causing fluctuation-induced transport are typically enhanced by gradients in properties such as plasma density.[5] One possible explanation for this transport barrier is that it is caused by the axial gradient in azimuthal electron velocity, which is maximized in the same region.[6] Support for this idea is provided by many fusion applications, such as tokamaks and stellarators, which exhibit similar confinement phenomena in regions of strong shear. It is believed that the anomalous conductivity caused by fluctuations is suppressed in regions where the flow is sheared due to the stretching and consequent decorrelation of turbulent eddies.[7]

An accurate description of the relation between flow shear and the transport barrier will allow not only more accurate simulations, but also a means to further optimize thruster performance. A steeper transport barrier will result in a narrower and stronger axial electric field, possibly decreasing plume divergence. Also, placement of the barrier may have an effect on propellant utilization efficiency. In order to numerically capture the transport barrier due to shear, an empirical model based on observations by the fusion community[8,9] and a simplified linear analysis[10] has been implemented in a radial-axial hybrid simulation of a Hall thruster. Section II provides descriptions of the numerical hybrid simulation and the shear transport model while Section III presents the results of the shear model through a comparison with other transport models and a discussion of the fitting parameters. A preliminary examination of the transportability of this model with a given set of fitting parameters to other simulations is also provided in Section III.

II. Numerical Model

A. Hybrid Simulation

The hybrid PIC simulation used for comparison with the linear analysis is a two-dimensional (radial-axial) hybrid model of the interior channel and near field region of a laboratory Hall thruster.[11,12] The simulated geometry corresponds to an annular thruster 8 cm in length, 1.2 cm in width, and with an outer diameter of approximately 9 cm. In the hybrid model the electrons are treated as a quasi-one-dimensional fluid while the heavy species are treated as discrete particles advanced in space using a particle-in-cell (PIC) approach. The two solutions are coupled assuming space charge neutrality.

The electron fluid is governed by the first three moments of the Boltzmann equation, as described by Fife.[13] The electron continuity equation is enforced through current continuity, where the instantaneous discharge current is determined in order to satisfy the potential boundary conditions at the anode and cathode. The electron momentum equation is solved in the two directions parallel and perpendicular to the magnetic field. Along magnetic field lines, infinite conductivity is assumed resulting in a balance between electric and pressure forces. In the perpendicular direction, an effective Hall parameter is used to determine the electron velocity in order to account for the anomalously high electron cross field conductivity relative to classical diffusion. Three separate models for the Hall parameter have been implemented in the simulation and will be examined in this paper: an empirical shear-based calculation, an experimentally-measured profile,[1] and a Bohm-type model.[14]

Imposing uniform temperature along magnetic field lines, a one dimensional energy equation is solved to calculate the electron temperature. The unsteady spatially varying electron energy equation includes thermal conduction and flow work as well as source and sink terms due to joule heating, ionization and heat loss to the channel walls. In addition to the electron cross field velocity description, heat conduction is also modelled using the experimentally measured anomalous conductivity. The electron temperature is coupled to the electric field through current continuity.

The axisymmetric heavy particle species are advanced in time through solution of their respective equations of motion in cylindrical coordinates. Due to the large Larmor radius of the ion species, the force produced by the magnetic field on the ions is neglected. Neutral injection occurs from the center of the anode, as well as from the boundaries of the plume to simulate background gas, with a distribution based on a one-way Maxwellian flux. Electron impact ionization of neutral particles is modelled using local densities and the electron temperature. Heavy particles which impact channel walls are assumed to reflect diffusely at the wall temperature, while in addition, ions are assumed to recombine into neutrals upon impact. Charge exchange collisions occur throughout the domain.

The simulation is initialized with approximately 500,000 neutral superparticles and 200,000 ion superparticles, where each superparticle represents between 10^8 and 10^{12} actual particles. The temperature profile and current are also initialized and used to calculate an initial electric field. The heavy particles are updated individually through a second-order solution of the equation of motion for each superparticle. Neutral particles are injected from the anode and plume based on the prescribed mass flow rate and background pressure, while charge exchange collisions are simulated using a DSMC approach. The electron temperature is updated using a fourth order Runge Kutta scheme satisfying the imposed boundary conditions of no heat transfer at the anode and prescribed temperature at the cathode. The computed temperature profile is used to update the potential, and the discharge current is modified as necessary to satisfy the potential boundary conditions. Due to the fast electron time scale relative to the ions and neutrals, the time step used for the electrons is 0.1 ns, while the heavy particles are advanced after several electron iterations with a time step of 25 ns. On a 3.8 GHz Pentium 4 processor, the simulation completes 625 s, or approximately 5-10 "breathing mode" cycles,[15] in two days.

B. Shear-Based Transport Model

Experimental measurements of the electron cross field mobility, an example of which is given in figure 1, illustrate that the effective Hall parameter, $\omega\tau_{\text{eff}}$, is considerably higher than the classical value in most regions of the Hall thruster channel.[1] An exception exists near the exit plane of the thruster where the transport approaches the classical value. As shown in figure 2, this region of decreased transport overlaps with a region of strong electron axial shear.[6] Similar transport barriers in the region of high shear have also been observed experimentally in fusion devices over the last two decades.[16,17]

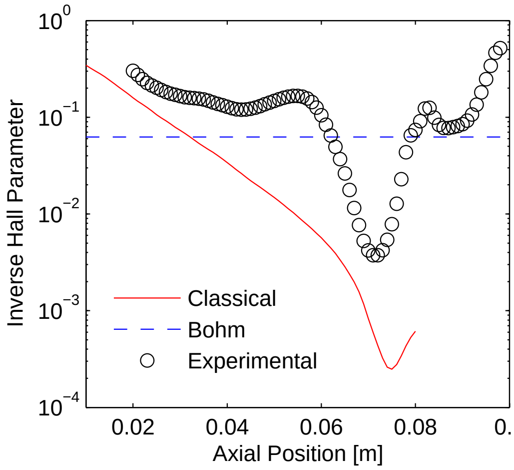

Figure 1. Experimental inverse Hall parameter is compared with the classical value based on experimental collision rates and the Bohm values at a discharge voltage of 200V.

Due to the importance of the transport barrier in fusion applications for reasons such as plasma confinement and reduction of heat loss, the phenomena of reduced transport due to electron shear has been extensively studied. It has been analytically shown that electron diffusion is decreased due to a reduction in the turbulent fluctuation amplitudes as well as a modification of the phase difference, or cross phase, between fluctuations in plasma properties which cause transport, such as plasma density and electron velocity.[18–21]

Qualitatively, the shear turbulence suppression mechanism is a result of the stretching and distortion of turbulent eddies caused by the position dependent velocity of fluid elements within the eddy. The distortion results in an effective decrease in the eddy lifetime, lowering the time scale from the eddy turnover time to the inverse shear rate, and a decrease in the correlation length in the direction of transport.[7] Also, it has been suggested that the shearing of the flow improves the overall stabilization of the system by coupling unstable modes to nearby stable modes leading to a reduction in transport.[22] The universal nature of the turbulence suppression mechanism extends to non-ionized fluids as well as plasmas. Although not common in hydrodynamics, a similar phenomenon is observed in large-scale turbulence in the stratosphere.[23]

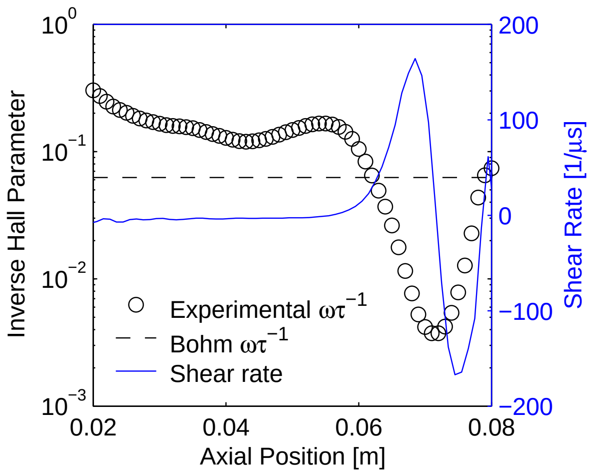

Figure 2. Experimental measurements of inverse Hall parameter and axial electron shear rate at 200V discharge voltage.

Due to the complicated nature of the nonlinear process, a number of different transport models have been suggested to describe this reduction of transport. The model examined in this paper is of the form:[8,9]

$$\omega\tau_{\text{eff}}^{-1} = \omega\tau_{\text{clas}}^{-1} + \omega\tau_{\text{nw}}^{-1} + \omega\tau_{\text{fluc}}^{-1}\left(\frac{1}{1+(C_1 s)^2}\right) \tag{1}$$

where $\omega\tau_{\text{clas}}$ is the classical Hall parameter based on electron neutral collisions, $\omega\tau_{\text{nw}}$ is the near wall term based on the electron collision rate with channel walls, $\omega\tau_{\text{fluc}}$ describes the transport due to fluctuations, and the shear rate, s, is given by:

$$s = \frac{du_{e,\theta}}{dz} = \frac{dE_z/B_r}{dz} \tag{2}$$

This form is consistent with a linearized calculation performed by Thomas.[10] Conventionally, the Bohm value of 16 is used for $\omega\tau_{\text{fluc}}$.[14] However, since the transport using this value was found to be too low in the radial-axial hybrid simulation, this term was treated as an adjustable fitting parameter. The coefficient C_1 represents the turbulence decorrelation time in the absense of shear, which is related to the growth rate of the instability causing transport. As this value is not known and may depend on a number of nonlinear effects, C_1 is also treated as a fitting parameter. At each timestep, the effective Hall parameter, $\omega\tau_{\text{eff}}$, is calculated using simulated plasma properties to compute $\omega\tau_{\text{clas}}$, $\omega\tau_{\text{nw}}$, and s.

At present, three simplifying assumptions are made to both reduce computational cost and increase numerical stability. First, the Hall parameter is only calculated along the center of the channel and assumed to be radially uniform. Second, the Hall parameter outside the channel is assumed to be constant at the value specified by the fitting parameter, $\omega\tau_{\text{fluc}}$. Lastly, the updating of the effective Hall parameter is under-relaxed, resulting in an instantaneous Hall parameter that contains remnant effects from the previous 1000 timesteps, or 25 μs. The effect of these assumptions on the results has not yet been carefully examined.

It should be noted that other forms for the reduction in transport have been suggested by the fusion community. The effect of a different empirical model in a radial-axial fully-kinetic Hall thruster simulation has been examined by Fox *et al.*[24] In this model, the ratio of transport with shear to the transport without shear is given by:[25]

$$1 - \frac{s}{C_2} \tag{3}$$

where C_2 is the maximum growth rate of the instability leading to transport.

A third empirical form states that the particle flux may be reduced by the following factor:[26]

$$1 - \frac{s^2}{C_3^2} \tag{4}$$

Future work will involve examining these forms to determine which most accurately describes the transport barrier observed in Hall effect thrusters.

III. Results and Discussion

A. Comparison of Transport Models

As a first step toward incorporating a shear-based model for electron cross field transport into the hybrid Hall thruster simulation, fitting parameters for the empirical form given by Equation 1 were chosen such that the initial computed Hall parameter resembled the experimentally measured profile for a discharge voltage of 200 V. This was determined by running the simulation using the experimental mobility and substituting the time-averaged output into the empirical form to determine which parameters most closely reproduced the experimental Hall parameter. However, when a shear-based conductivity model was implemented using these fitted constants, the plasma properties used to optimize the parameters were modified due to the change in electron transport.

Generally speaking, introduction of the shear-based transport mechanism caused the axial gradient in azimuthal electron velocity to decrease using the chosen constants. Due to the coupled nature of all plasma properties, the decrease in the flow shear was accompanied by a reduction of the transport barrier as well as a broadening of the potential and electron temperature. This resulted in an overall increase in current and plasma density due to the increased mobility. In order to counteract these effects, new fitting parameters were chosen after each successive run to try and better predict the experimentally observed transport barrier and simulated properties.

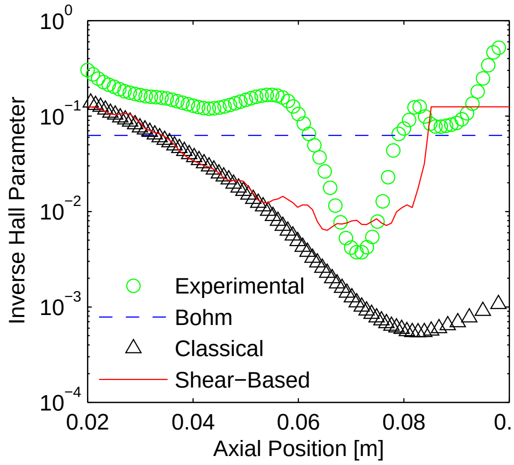

Figure 3. Shear-based inverse Hall parameter is compared with the classical value based on simulated collision rates, the Bohm value, and experimental measurements at a discharge voltage of 200V.

While the initial fitting parameters chosen based on the experimental mobility were $\omega\tau_{\text{fluc}} = 10$ and $C_1 = 3 \times 10^{-8}$, the improved, though not necessarily optimum, parameters were found to be $\omega\tau_{\text{fluc}} = 8$ and $C_1 = 16 \times 10^{-8}$. The shear-based Hall parameter computed using the updated constants is compared with the experimentally measured, classical, and Bohm Hall parameters in figure 3. Note that the inverse Hall parameter outside the channel is fixed to a constant Bohm-like value. One issue presently being examined is the breadth of the suppression due to shear. While one might expect the Hall parameter to be approximately Bohm near the anode, in this region, numerical noise combined with an overall low magnetic field leads to large azimuthal electron velocities and correspondingly large shear values.

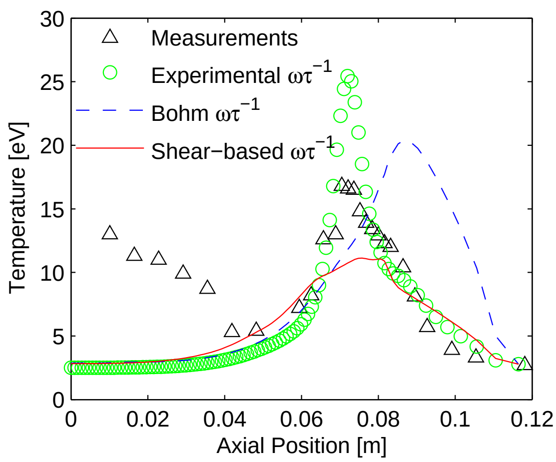

Figure 4. Comparison between measured and simulated electron temperature using Bohm, experimental, and shear-based models for electron transport.

The Hall parameter profile computed using the initial parameters of $\omega\tau_{\text{fluc}} = 10$ and $C_1 = 3 \times 10^{-8}$ was found to be less suppressed and more Bohm-like. As a result, the computed plasma properties with these parameters more closely resembled the results using a Bohm mobility with the maximum in temperature and electric field occurring outside the channel. The plasma properties calculated using the new parameters of $\omega\tau_{\text{fluc}} = 8$ and $C_1 = 16 \times 10^{-8}$ more closely resemble the measured plasma properties. As shown by figure 4, the experimental mobility most accurately captures the shape of the electron temperature profile. Due to the broadness of the transport barrier, the shear model predicts a wider profile, with a peak temperature lower than the experimental value. Other factors such as energy loss to the walls due to anisotropic electron velocity distributions may also play a role in determining the overall temperature. Relative to the Bohm-type transport model, the Hall parameter of which contains no barrier to electron motion, the shear model more accurately captures the location of the peak temperature.

Figure 5 illustrates the effect of Bohm, experimental, and shear-based transport models on the electric potential. The steep temperature profile produced by the experimental mobility as shown in figure 4 produces a potential drop which is steeper than experimental observations resulting in a high electric field. While the Bohm mobility produces similar electric fields to experiments, the potential drop occurs farther downstream than expected. The shear model, on the other hand, predicts moderate electric fields occurring approximately in the location experimentally observed. It should be noted that while the shear-based transport model predicts the potential reasonably well, the corresponding ion acceleration is found to be too broad.

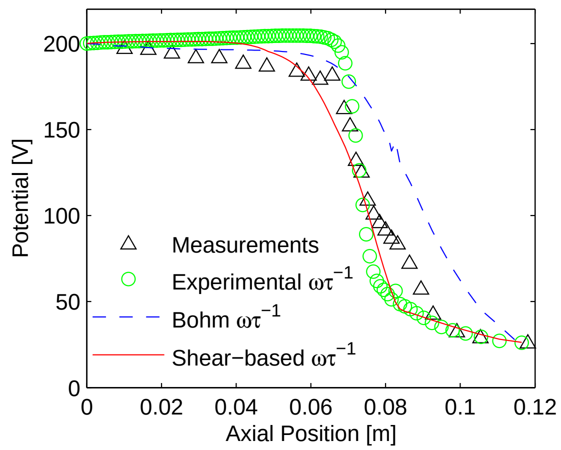

Figure 5. Comparison between measured and simulated electron potential using Bohm, experimental, and shear-based models for electron transport.

B. Sensitivity of Fitting Parameters

As previously noted, the two fitting parameters, C_1 and $\omega\tau_{\text{fluc}}$, were chosen somewhat arbitrarily to produce reasonable agreement with experimental measurements. While it is true that certain combinations of parameters produce poor agreement, the constants chosen for the results presented in Section IIIA are by no means the only feasible choice. In fact, overall the results are relatively insensitive to these constants. Variations from the chosen values of $\omega\tau_{\text{fluc}} = 8$ and $C_1 = 16 \times 10^{-8}$ have been implemented in the hybrid simulation to ascertain the effect that these parameters have on plasma properties.

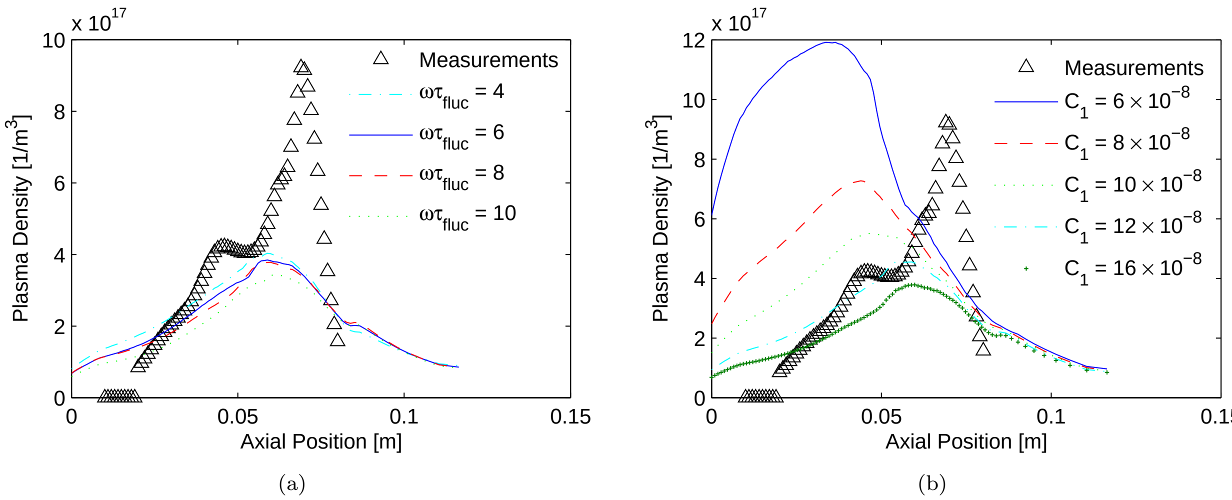

Figure 6. Trend observed in plasma density due to variation of fitting parameters, (a) $\omega\tau_{\text{fluc}}$ and (b) C_1, at discharge voltage of 200V. In (a) C_1 is held constant at 16×10^8 while in (b) $\omega\tau_{\text{fluc}}$ is held constant at 8.

The sensitivity to adjustments of the parameters has been found to be relatively small for properties such as potential, electron temperature, and neutral and ion velocities. The plasma property most sensitive to alteration of these parameters is the plasma density. The variations in plasma density due to changes in $\omega\tau_{\text{fluc}}$ and C_1 are illustrated in figure 6. In this figure, results are averaged over 100 μs or approximately one breathing-mode cycle. While the chosen value of C_1 in the empirical model seems to have a considerable effect on plasma density, the effect of the base fluctuation Hall parameter, $\omega\tau_{\text{fluc}}$, found to be fairly small.

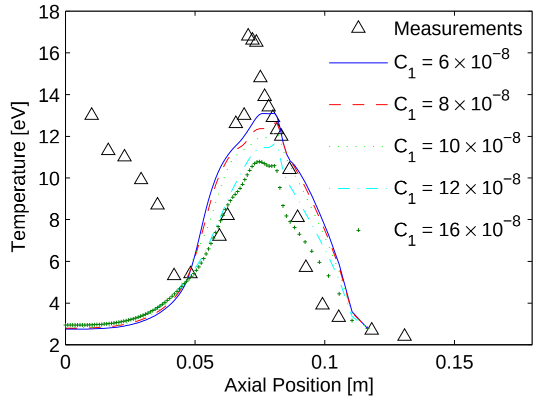

Figure 7. Trend observed in electron temperature due to variation of fitting parameter, C_1, at discharge voltage of 200V.

As shown in figure 6(a), the plasma density increases slightly as $\omega\tau_{\text{fluc}}$ is decreased. This is expected since a lower baseline Hall parameter corresponds to a higher mobility. The increased conductivity of electrons leads to a higher current density which produces more joule heating. The increased heating causes higher temperatures and larger ionization rates leading to an increased plasma density. However, as illustrated by figure 6(a), this effect is small.

As shown in figure 6(b), the plasma density also increases as C_1 is decreased. Based on the form of Equation 1, this is expected since the fluctuation induced transport is further suppressed as the value of C_1 is increased. However, while changes in the C_1 fitting parameter produce large effects on the plasma density, both in the magnitude and location of the peak value, the effects are less significantly observed in other plasma properties such as electron temperature and potential. As shown in figure 7, due to the increased turbulence suppression which slows down the electron cross field transport resulting in lower joule heating, electron temperatures decrease as C_1 is increased. The broadening and increase of electron temperature profiles at low values of C_1 leads to increased ionization closer to the anode, shifting the location of the peak plasma density upstream and resulting in higher peak densities.

C. Transportability of Shear-Based Model

While, physically, it is expected that the values of C_1 and $\omega\tau_{\text{fluc}}$ will vary for different operating conditions and thruster geometries, an attempt has been made to examine the transportability of these parameters to simulations other than the one for which they were optimized. Although the parameters are likely dependent on plasma properties and characteristics of the instability causing transport, the hope is that they will not be highly sensitive to these variables resulting in an empirical model which can be used to describe the transport barrier in thrusters for which an experimental mobility has not been measured.

As a starting point, the empirical shear based transport model developed in the previous sections was introduced into a hybrid simulation with the same geometry and magnetic field configuration, but lower operating voltage than used in Section IIIA. Since experimental data has been measured at 160 V in addition to 200 V,[27] the empirical model with the improved fitting parameters of $\omega\tau_{\text{fluc}} = 8$ and $C_1 = 16 \times 10^{-8}$ was implemented at a 160 V discharge voltage.

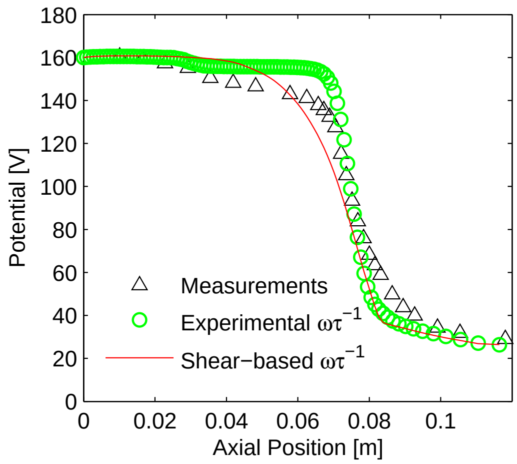

Figure 8. Comparison between measured and simulated electron potential using experimental and shear-based models for electron transport at a discharge voltage of 160 V.

As shown in figure 8, the shear model for electron transport predicts the drop in electric potential at a discharge voltage of 160 V reasonably well. Using the empirical model, the potential drop is more gradual than predicted using the experimental mobility, producing electric field estimates in better agreement with laboratory measurements. However, using these constants, chosen based on the 200 V operating condition, the peak simulated electron temperature at 160 V is a factor of 2 lower than experimental measurements (8 eV instead of 16 eV). As demonstrated in Section IIIB, the plasma density is highly sensitive to electron temperature resulting in a peak plasma density at 160 V more than an order of magnitude lower than predicted by experimental observations.

A second method of evaluating the transportability of the empirical fitting parameters has been to implement the shear-based model in a similar hybrid radial-axial simulation of a bismuth Hall thruster. In addition to the differing propellant, the simulation also uses a slightly different geometry with a channel length of 2.4 cm instead of the 8 cm channel analyzed in previous sections. As this thruster is still in the development stage, experimental data of plasma properties have not yet been collected. Therefore, rather than being used to evaluate the accuracy of the shear-based transport model and the chosen fitting coefficients, this exercise illustrates the transportability of the model in the sense of numerical robustness. For Hall thruster models intended to simulate new devices lacking any experimental data, the ability of the assumed transport model to sustain the numerical discharge is critical in the early development stages of the simulation.

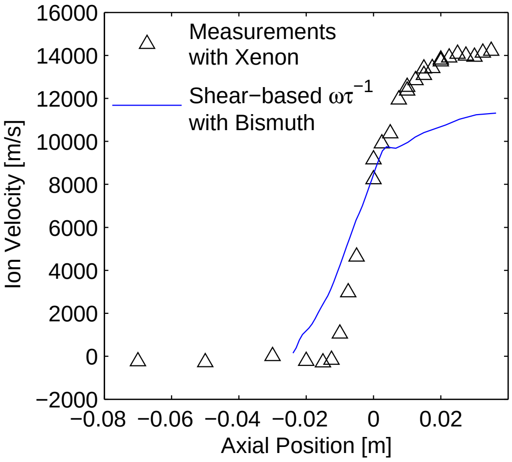

Figure 9. Comparison of measured xenon ion velocity with simulated bismuth ion velocity using shear-based model from xenon simulation. Exit plane located at zero.

Implementation of the shear-model for electron transport in the bismuth Hall thruster simulation using constants determined from the xenon hybrid code was accomplished without numerical difficulty. The bismuth code underwent an initial transient lasting approximately one breathing mode cycle in which the electron current fell to 0.07 A and rose to 4 A before settling to an average value of approximately 2 A ± 0.5 A. Although the fitting parameters in the shear-based transport model may not be ideal for the bismuth thruster, the use of this model provided qualitatively reasonable plasma properties. Figure 9 shows a comparison between the experimentally measured xenon axial ion velocity in the 8 cm cylindrical Hall thruster at 200 V and the simulated bismuth profile for the shorter channel with the same number flow rate. Unlike previous figures, in this graph the exit plane is indicated by an axial position of 0 m to account for the differing channel lengths. As expected bismuth reaches a lower maximum axial ion velocity than xenon across the same potential drop due to its larger mass.

Table 1 illustrates the performance characteristics between the xenon and bismuth hybrid simulations at a discharge voltage of 200 V. In addition to differing propellents and channel lengths, the bismuth simulation uses a larger mass flow rate to simulate the same number flux and does not include charge exchange and background pressure, as is done in the xenon simulation.

In table 1, thrust is calculated by summing the electric force on all the ion superparticles. In addition to providing more thrust per ion accelerated over the same potential drop, the bismuth thruster has the added advantage of a lower ionization potential resulting in a higher plasma density and propellant efficiency. At locations near the anode of the bismuth thruster, the simulated plasma density is found to be an order of magnitude higher than the corresponding xenon value, leading to a higher total discharge current. Although one might expect the bismuth specific impulse to be lower than that for xenon due to the lower exhaust velocity, the propellant utilization of the simulated bismuth thruster is sufficiently high that the I_{sp}, computed by dividing total thrust by mass flow rate and gravity, is found to be higher for bismuth. Similarly, due to the higher thrust per particle and a larger ionization rate, the simulated total efficiency is found to be a factor of 2 larger using the bismuth propellant.

Table 1. Comparison of simulated performance parameters from xenon and bismuth 2D hybrid Hall thruster simulations.

	Bi	Xe
Thrust [N]	0.042	0.022
Current [A]	1.90	1.61
I_{sp} [s]	1331.9	1104.1
Total Efficiency	0.716	0.364

IV. Summary

Motivated by the observations and analytical work of the fusion community, an empirical model for electron cross field transport has been implemented in 2D hybrid Hall thruster simulations based on the axial shear rate of the electron fluid. It is believed that the shearing of the fluid, caused by electric and magnetic field gradients, reduces the fluctuation-enhanced anomalous transport through stretching and distortion of turbulent eddies.

It has been shown that implementation of a shear-based transport barrier, which is computed locally and updated continuously, produces reasonable agreement with laboratory measurements. Despite a broader simulated transport barrier than experimentally observed, simulations using the shear-based approach produce similar profiles for electron temperature and potential as with use of the experimental mobility. In all cases, the empirical shear-based transport model more accurately predicts plasma properties than a simple Bohm Hall parameter lacking any barrier to cross-field transport.

In order to evaluate the utility of this method, which relies on the unknown fitting parameters $\omega\tau_{\text{fluc}}$ and C_1, an assessment was made of the sensitivity of the results to changes in these coefficients. For the specific conditions examined, it was found that plasma properties were fairly insensitive to the base value of anomalous transport, $\omega\tau_{\text{fluc}}$, and more largely dependent on the constant, C_1, which is likely related to the growth rate of the instability producing transport.

An attempt has also been made to evaluate the utility of the empirical model through examination of the transportability of the model itself and the fitting parameters to different operating conditions and thruster geometries. Simulations for the same thruster at 160 V using the coefficients chosen at 200 V reproduced the potential drop reasonably well, but underestimated the plasma density by an order of magnitude, suggesting that the parameters likely have a slight dependence on operating conditions. Also, the shear-based model has been incorporated into a simulation of a bismuth thruster currently being developed. Although experimental data is not available for comparison, results are in qualitative agreement with expectations. In the future, attempts will be made to incorporate the empirical shear-based transport model into simulations of other laboratory thrusters with extensive experimental data, such as the SPT 100.

Acknowledgments

This research was supported in part by the U.S. Air Force Office of Scientific Research. Stipend support for M. Scharfe was provided by the Stanford Graduate Fellowship Program.

References

[1]Meezan, N., Hargus, W., and Cappelli, M., "Anomalous electron moblity in a coaxial hall plasma discharge," *Physical Review E*, Vol. 63, 2001, pp. 026410.

[2]Gascon, N., Dudeck, M., and Barral, S., "Wall material effects in stationary plasma thrustser. I. Parametric studies of an SPT-100," *Physics of Plasmas*, Vol. 10, No. 10, 2003, pp. 4123–4136.

[3]Barral, S., Makowski, K., Peradzynski, Z., Gascon, N., and Dudeck, M., "Wall material effects in stationary plasma thrusters II: Near wall and inner-wall conductivity," *Physics of Plasmas*, Vol. 10, No. 10, 2003, pp. 4137.

[4]Janes, G. and Lowder, R., "Anomalous Electron Diffusion and Ion Acceleration in a Low Density Plasma," *Physics of Fluids*, Vol. 9, No. 6, 1966, pp. 1115–1123.

[5]Wootton, A., Carreras, B., Matsumoto, H., McGuire, K., Peebles, W., Ritz, C., Terry, P., and Zweben, S., "Fluctuations and anomalous transport in tokamaks," *Physics of Fluids B*, Vol. 2, No. 12, 1990, pp. 2879–2903.

[6]Cappelli, M., Meezan, N., and Gascon, N., "Transport Physics in Hall Plasma Thrusters," *Proceedings of the 40th Aerospace Sciences Meeting*, No. AIAA-2002-0485, American Institute of Aeronautics and Astronautics, 2002.

[7]Terry, P., "Suppression of turbulence and transport by sheared flow," *Reviews of Modern Physics*, Vol. 72, No. 1, 2000.

[8]Jachmich, S., Schoor, M. V., and Weynants, R., "On the causality between transport reduction and induced electric fields in the edge of a tokamak," *Proceedings of the 39th Conference on Plasma Physics and Controlled Fusion*, Vol. 26B, European Physical Society, 2002.

[9]Hahm, T., "Physics behind transport barrier theory and simulations," *Plasma Physics and Controlled Fusion*, Vol. 44, 2002, pp. A87–A101.

[10]Thomas, C., *Anomalous Electron Transport in the Hall-Effect Thruster*, Ph.D. thesis, Stanford University, California, Oct. 2006.

[11]Fernandez, E., Cappelli, M., and Mahesh, K., "2D simulations of hall thrusters," *CTR Annual Research Briefs*, 1998, pp. 81.

[12]Scharfe, M., Gascon, N., Cappelli, M., and Fernandez, E., "Comparison of Hybrid Hall Thruster Model to Experimental Measurements," *Physics of Plasmas*, Vol. 13, No. 8, 2006.

[13]Fife, J., *Nonlinear hybrid-PIC modeling and electrostatic probe survey of hall thrusters*, Ph.D. thesis, Massachusetts Institute of Technology, 1998.

[14]Bohm, D., Burhop, E., and Massey, H., *The Characteristics of Electrical Discharges in Magnetic Fields*, McGraw Hill, New York, NY, 1949, p. 13.

[15]Boeuf, J. and Garrigues, L., "Low frequency oscillations in a stationary plasma thruster," *Journal of Applied Physics*, Vol. 84, 1998, pp. 3541.

[16]Ritz, C., Lin, H., Rhodes, T., and Wootton, A., "Evidence for Confinement Improvment by Velocity-Shear Suppression of Edge Turbulence," *Physical Review Letters*, Vol. 65, No. 20, 1990.

[17]Synakowski, E., Batha, S., Beer, M., Bell, M., Bell, R., Budny, R., Bush, C., Efthimion, P., Hahm, T., and Hammet, G., "Local transport barrier formation and relaxation in reverse-shear plasmas on the Tokamak Fusion Test Reactor," *Physics of Plasmas*, Vol. 4, No. 5, 1997, pp. 1736–1744.

[18]Biglari, H., Diamond, P., and Terry, P., "Influence of sheared poloidal rotation on edge turbulence," *Physics of Fluids B*, Vol. 2, No. 1, 1990.

[19]Zhang, Y. and Mahajan, S., "Edge turbulence scaling with shear flow," *Physics of Fluids B*, Vol. 4, No. 6, 1992, pp. 1385–1387.

[20]Ware, A., Terry, P., Diamond, P., and Carreras, B., "Transport reduction via shear flow modification of the cross phase," *Plasma Physics and Controlled Fusion*, Vol. 38, 1996, pp. 1343–1347.

[21]Terry, P., Newman, D., and Ware, A., "Suppression of Transport Cross Phase by Strongly Sheared Flow," *Physical Review Letters*, Vol. 87, No. 18, 2001.

[22]Burrell, K., "Effects of ExB velocity shear and magnetic shear on turbulence and transport in magnetic confinement devices," *Physics of Plasmas*, Vol. 4, No. 5, 1996.

[23]Terry, P., "Does flow shear suppress turbulence in nonionized flows?" *Physics of Plasmas*, Vol. 7, No. 5, 2000, pp. 1653–1661.

[24]Fox, J., Batishcheva, A., Batishchev, O. V., and Martinez-Sanchez, M., "Adaptively Meshed Fully-Kinetic PIC-Vlasov Model for Near Vacuum Hall Thrusters," *Proceedings of the 42nd Aerospace Sciences Meeting and Exhibit*, No. AIAA-2006-4324, American Institute of Aeronautics and Astronautics, Washington, DC, 2006.

[25]Waltz, R., Staebler, G., Dorfand, W., Hammett, G., Kotschenreuther, M., and Konings, J. A., "A gyro-Landau-fluid transport model," *Physics of Plasmas*, Vol. 4, No. 7, 1997, pp. 2482–2496.

[26]Ware, A., Terry, P., Carreras, B., and Diamond, P., "Turbulent heat and particle flux response to electric field shear," *Physics of Plasmas*, Vol. 5, No. 1, 1998, pp. 173–177.

[27]Hargus, W., *Investigation of the plasma acceleration mechanism within a coaxial Hall thruster*, Ph.D. thesis, Stanford University, 2001.